

Carrier-Mediated Active Transport Models by Affinity-Switching Strategy

Sung-Kil LEE and Koji ARAKI*
Institute of Industrial Science, University of Tokyo,
7-22-1 Roppongi, Minato-ku, Tokyo, 106, Japan

Active transport is one of the essential function of biological membrane transport systems, in which substrates are transported from lower to higher concentration side against their concentration gradient. In this article, we describe photo- and pH-induced active transport models by designing the functional carriers based on the affinity-switching strategy.

1. Introduction

Biological membrane transport system has a variety of function of importance. Among them, active transport is one of the representative high functionality of the biological transport systems. As a model of the biological membrane transport, carrier-mediated transport across an artificial membrane has been investigated extensively.¹⁾ Since operation of active transport requires other free energy source, it is essential to develop the carrier that can utilize other free energy source in order to design artificial active transport.

Most of the carrier-mediated transport of ionic species involve ion-exchange processes at the membrane interfaces. To achieve high transport efficiency, high substrate affinity of the carrier is required in the extraction process, while low affinity is favorable for the release process. Therefore, affinity switching of the carrier during the transport process can achieve highly efficient transport, leading to active transport when alteration of the affinity is sufficiently large.²⁾

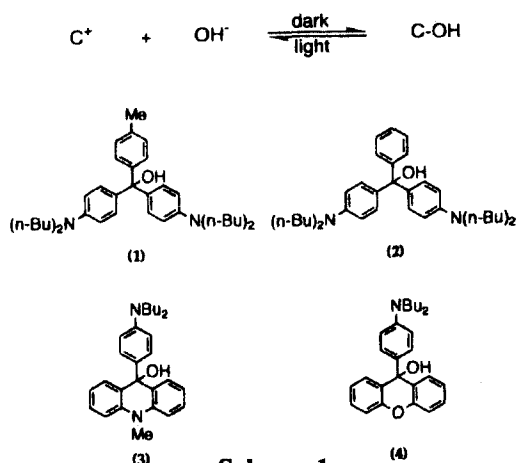
In this article, we will show brief overview of our recent research on the carrier-mediated active transport systems based on the affinity-switching strategy.

2. Photo-Driven Active Transport Systems

Switching the affinity of the carrier by photo-irradiation can induce photo-driven active transport, which can be a primary active transport model. Several groups have reported photoresponsive carriers that can change their substrate affinity.³⁾ However, most of them failed to demonstrate the photo-driven active transport. To induce active transport, many factors in addition to the photoresponsibility of the carrier have to be tuned properly. In this section, we studied the factors affecting the performance of anion transport by photochemically generated triaryl cation in order to obtain a better understanding of the active transport system.

2.1 Photo-driven Active Transport of Anions Mediated by Triarylmethanol⁴⁾

Triarylmethanol (C-OH) derivatives are selected as the photoresponsive anion carriers. They undergo reversible dissociation into triaryl cation (C⁺) and hydroxide ion (OH⁻) by photo-irradiation (Scheme 1). Neutral C-OH in the organic phase does not bind



Scheme 1

anions, while photo-generated C^+ has the ability to extract anion from the aqueous phase.

When *p*-toluenesulfonate (tosylate) was used as a substrate, practically no active transport of tosylate was observed with bis [4-(*n*-butylamino)phenyl]-4'-methylphenylmethanol (**1**), which was ascribed to the slow release of tosylate into the receiving phase. (Fig. 1 (a)) To accelerate the release process, more hydrophilic bromide was used as the substrate which is expected to reduce the

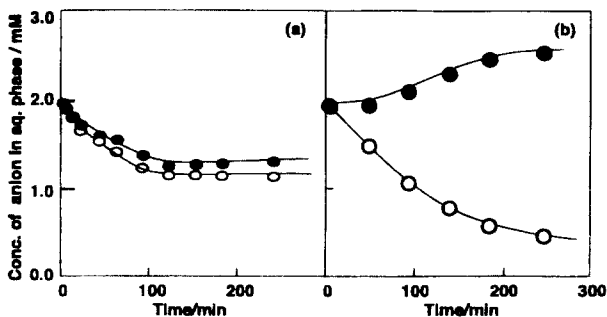


Fig. 1 Transport of Anions by Triaryl Alcohol (**1**)
(a) *p*-toluenesulfonate and (b) bromide.

stability of the ion pair C^+X^- in the organic membrane phase. Photo-driven active transport was induced by **1** upon photoirradiation from the illuminated side to the dark side. (Fig. 1 (b)).

Photo-dissociated form (C^+) of 9(10*H*)-bis[4-(*n*-butylamino)phenyl]-10-methylacridin-9-ol (**3**) and 9-bis[4-(*n*-butylamino)phenyl]-xanthen-9-ol (**4**) have shorter life-times than that of **1** and therefore, accelerate the release process. The carrier **3** mediated efficient photo-driven active transport of tosylate. However, the carrier **4** showed poor transport ability. Because stability of the cation form of carrier **4** was too low to induce sufficient extraction of tosylate.

Thus, it is shown that the photo-driven active transport of anions by triaryl cations can be achieved only after fine tuning of hydrophilic/hydrophobic nature of the anions or by controlling the stability of the triaryl cation. The results demonstrated that the proper tuning of the transport system is essential to design artificial active transport system.

3. pH-Induced Up-hill Transport by a Functional Metal Complex⁵⁻⁸⁾

As a secondary active transport model, we designed a pH-induced efficient up-hill transport system. For this purpose, we applied the affinity-switching concept for development of a novel complex-type anion carrier.

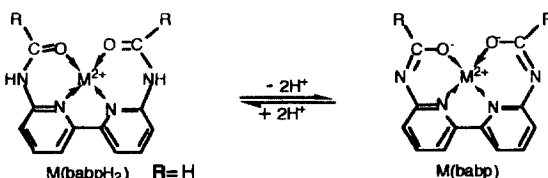
3.1 Design of functionality metal complexes as a functional carrier.

Divalent metal complexes of 6,6'-bis(benzoylamino)-2,2'-bipyridine have the properties suitable for the functional anion carriers, and show excellent chemical and thermal stability.⁹⁾ Between cationic metal center and anions, electrostatic and coordination interactions are expected to operate. These intermolecular interactions are relatively strong, and operate effectively not only in organic media but also in aqueous solutions. Therefore, high anion affinity can easily be attained by the complex-type carrier. Total charge of a cationic complex can be reduced by introduction of negative charge to the ligand moiety. Electrostatic interaction with anions diminishes when the net charge of the complex becomes neutral.

Reversible dissociation of the amide moieties of the ligand provides efficient way to regulate the total charge of the complex, and, therefore, the anion affinity (Scheme 2).

To adjust the hydrophobic nature of the complex, we introduced *n*-hexyl groups to the parent complex and examined the properties of the Cu(II) and Ni(II) complexes of 6,6'-bis(4-hexylbenzoylamino)-2,2'-bipyridine (LH_2).

Addition of small amounts of methanolic NaOH solution to the MLH_2^{2+}/CH_2Cl_2



Scheme 2

solution caused spectral change (Fig. 2). The Cu(II) complex showed clear two-step spectral change (Fig. 2 (a)), but the Ni(II) complex, NiLH_2^{2+} , showed one-step spectral change (Fig. 2 (b)). The observed spectral change is ascribed to the step wise deprotonation of the Cu(II) complex (Scheme 3 (i)) through a mono-deprotonated complex, CuLH^+ into the fully-deprotonated complex, CuL . While, in the case of the Ni(II) complex, NiLH_2^{2+} , simultaneous deprotonation of the two amide units directly converted the non-deprotonated complex to the fully-deprotonated form (Scheme 3 (ii)). Deprotonation of the amide units of the complex was confirmed to be reversible by repeated addition of methanolic HCl and NaOH.

Electronic spectra of the complexes were measured in the presence of tetra-*n*-butylammonium (TBA) bromide, *p*-toluenesulfonate (tosylate) and thiocyanate (SCN^-) in CH_2Cl_2 at 20°C. The spectral changes were observed only for the non-deprotonated complexes when SCN^- was present in the solutions. In the case of the cationic complex in the non-deprotonated form, the complex bears two nitrate molecules as counter anions. Addition of poor coordinating anions, bromide and tosylate, did not affect the spectra of the non-deprotonated complex, but highly coordinating SCN^- caused clear spectral change. In the case of the neutral complex in the deprotonated form, no electrostatic interaction with anion is expected. Indeed, presence of any of the TBAsalts did not cause any detectable change in the electronic spectra of CuL and NiL . No spectral change was observed even with SCN^- having high coordination ability. This poor axial coordination of SCN^- to the complex is in good agreement with the fact that ML has stronger square-planar ligand field as evidenced by its blue-shifted d-d absorption band. Thus, it is confirmed that the cationic non-deprotonated complex has high SCN^- affinity, while the neutral fully-deprotonated complex shows poor anion affinity. Reversible amide-deprotonation caused drastic alteration of the anion affinity of the carrier complex.

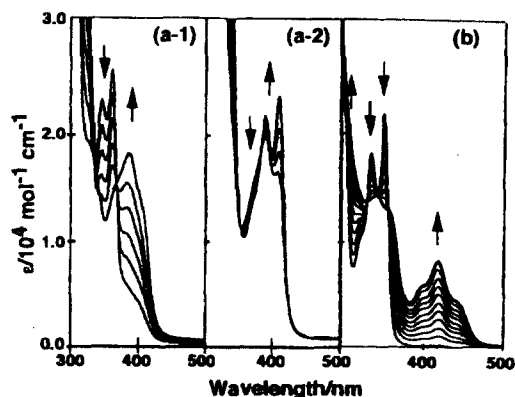
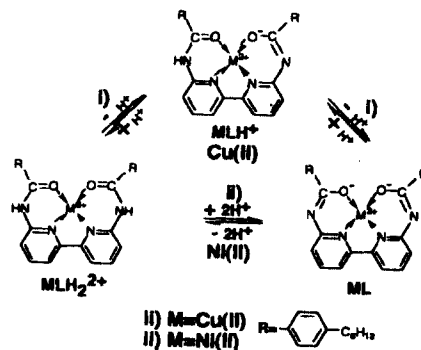


Fig. 2 Electronic Spectra of LH_2 and its (a)Cu(II) and (b) Ni(II) complexes in dichloromethane at 20°C. Spectral change of MLH_2^{2+} upon addition of small amounts of methanolic NaOH, where $[\text{NaOH}]/[\text{Complex}]$ molar ratios were (a-1) 0-1, (a-2) 1-2 and (b) 0-2.



Scheme 3

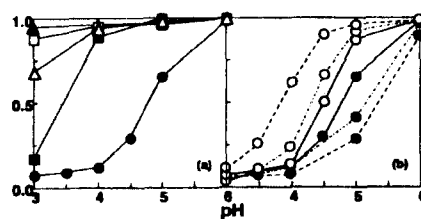


Fig. 3 PH profiles of the molar fraction of NiL in the organic layer after mixing with aqueous buffer solutions containing different (a) type of sodium salts and (b) NaSCN concentrations.

(a) Type of sodium salts (1.0×10^{-2} mol dm^{-3}): \triangle —: no salt, \bullet —: NaSCN , \blacksquare —: Nap-tol, \triangle —: NaClO_4 , and \square —: NaBr .
 (b) NaSCN concentrations: \circ —: 1.0×10^{-3} , \circ —: 3.0×10^{-3} , \circ —: 5.0×10^{-3} , \bullet —: 1.0×10^{-2} , \bullet —: 2.0×10^{-2} and \bullet —: 4.0×10^{-2} mol dm^{-3} .

3.2. pH-Induced up-hill transport of anions by the functional metal complex carrier.

Solute equilibria between aqueous and organic layers were studied in the two-phase system. Figure 3 shows pH profiles of the molar fraction of the Ni(II) complex in the deprotonated form in the organic layer. The results indicated that deprotonation of the complex in the organic layer was controlled by the pH, type of the anions, and the anion concentration of the aqueous buffer solutions.

Since no leakage of the complex into the aqueous layer was observed, apparent solute equilibria of the SCN⁻ system can be given as follows (1);

$$K_{app} = \frac{[\text{Ni}(\text{LH}_2)(\text{SCN})_2]_{org}}{[\text{SCN}^-]_{aq}^2 [\text{H}^+]_{aq}^2 [\text{NiL}]_{org}} \quad (1)$$

or

$$\log K_{app} = 2\text{pH} - 2\log [\text{SCN}^-]_{aq} + \log ([\text{Ni}(\text{LH}_2)(\text{SCN})_2]_{org}/[\text{NiL}]_{org})$$

where K_{app} ($\log K_{app}=13.6$) is the equilibrium constant and suffix aq or org indicates aqueous or organic layer, respectively. Lower pH or higher SCN⁻ concentration of the aqueous layer increases the molar fraction of the cationic non-deprotonated complex, showing that the reversible deprotonation of the complex in the organic membrane can be controlled by the external aqueous layer.

Transport experiments were carried out at 20°C using a three phase systems, where two aqueous buffer layers I and II (aq. I (pH3-5) and II (pH6)) were identical in their volume and initial SCN⁻ concentration, and were separated by the organic layer containing NiLH₂²⁺. The results are shown in Fig. 4. It is worth noting that only a small pH difference of two is sufficient to mediate efficient up-hill transport of SCN⁻. During the transport experiments, quantitative coupling of SCN⁻ transport with symport of proton was observed, which mediated the efficient pH-driven up-hill transport of SCN⁻. The transport mechanism of this system is illustrated in Scheme 4.

Lipophilic tosylate was also transported across the organic layer, but hydrophilic bromide was not transported at all. When tosylate and SCN⁻ were present simultaneously in the aqueous layers, SCN⁻ was selectively transported, showing that the coordination ability is the critical factor for the transport selectivity.

The Cu(II) complex of LH₂ also mediated the efficient and selective up-hill transport of anions by coupling with the pH difference across the liquid mem-

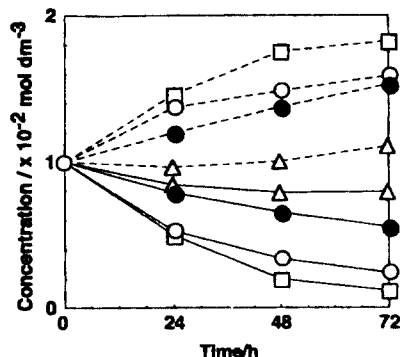
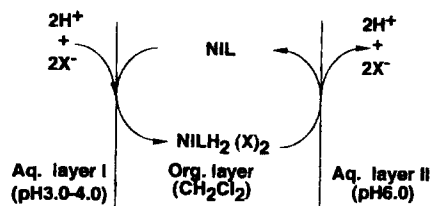


Fig. 4 Time course of the SCN⁻ concentration of the aqueous layer I (—) and II (---) during the SCN⁻ transport by NiLH₂²⁺ (1.11×10^{-4} mol dm⁻³) in the three-phase system at 20°C. Initial concentration of SCN⁻ in both aqueous layers were 1×10^{-2} mol dm⁻³. The layer II was set at pH6.0, while pH of the layer I was 3.0 (□), 4.0 (○) and 5.0 (△). For comparison, the SCN⁻ transport by CuLH₂²⁺ from the pH4.0 aqueous layer I under similar conditions (●) was also shown in the figure.



Scheme 4

brane. Thus, a novel complex-type carrier we developed showed excellent ability to induce up-hill transport of anions, which requires only the pH difference of two in order to generate coupled flow of SCN⁻.

3.3. Up-hill transport of biomolecules by the Ni(II) complex.

We extended this affinity-switching strategy further to the transport of biologically important substrates that have metal coordination site. Since deprotonation of the amide unit of the complex can switch not only the electrostatic interaction but also coordination interaction with the substrate, up-hill transport of the substrate that have coordination ability can be designed. For this purpose, an amino acid derivative, carbobenzoxy-histidine (Cbz-His) having imidazole as the coordination site, was selected as the substrate.

We tested the up-hill transport of Cbz-His by the Ni(II) complex of LH₂ at 20°C. Experimental conditions were essentially the same as those reported in the previous section. Two aqueous buffer solutions I and II contained same concentration of Cbz-His and NaClO₄, which were separated by the organic NiLH₂²⁺ layer. The results shown in Fig. 5 demonstrated that the carrier complex induced up-hill transport of Cbz-His. No transport of Cbz-His was observed without NiLH₂²⁺ in the organic layer or pH difference between two aqueous layers. Therefore, it is clear that the NiLH₂²⁺ is the carrier that induced up-hill transport of Cbz-His by coupling with the pH-difference across the membrane. Without NaClO₄, no practical up-hill transport was observed at all. From the synergistic effect of NaClO₄ observed for uptake of Cbz-His, role of NaClO₄ can best be interpreted as a lipophilic but weak coordinating counter anion that helps extraction of hydrophilic Cbz-His into the organic layer. Since many biomolecules have metal coordination sites in their structure, the results will open wide applicability for construction of artificial up-hill transport of biologically important molecules.

4. Conclusion

Through the results we presented here, design of the carrier based on the affinity switching concept is the practical and effective method to develop artificial active transport system. Functionality of the biomembrane transport system is still far away from the current level of artificial active transport system. However, the carriers that have much higher functionality can be designed and developed by introducing the concept of molecular recognition and/or enzyme-like activity of the metal complexes. In a near future, we believe that the artificial membrane transport by the affinity switching concept will be able to mimic some of the high functions that the biomembrane transport systems have.

References

- 1) J.-M. Lehn, " *Supramolecular Chemistry: Concepts and Perspectives* ", ed by C. St. Cooper, VCH, Weinheim, 1995.
- 2) M. Seno and K. Araki, in *New Functionality Materials*, eds. T. Tsuruta M. Seno and M.

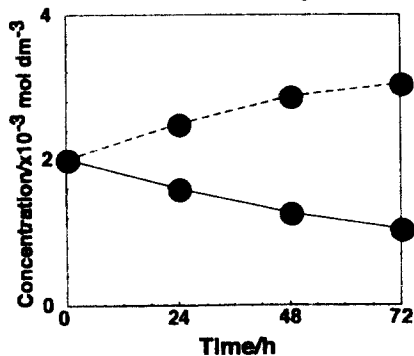


Fig. 5 Time course of the Cbz-His concentration in the aqueous layer I (pH 3.0, —) and II (pH 10.0, ----) during the up-hill transport across the CH₂Cl₂ layer mediated by NiLH₂²⁺ ($2.0 \times 10^{-4} \text{ mol dm}^{-3}$) at 20°C. Initial concentrations of Cbz-His in both aqueous layers were $2 \times 10^{-3} \text{ mol dm}^{-3}$.

Doyama, Elsevier Science Publishers, Amsterdam, 1993, Vol. C, pp.465.

- 3) (a) I. Yamashita et al., *Tetrahedron Lett.*, **1980**, 541. (b) S. Shinkai, K. Shigematsu, Y. Kusano and O. Manabe, *J. Chem. Soc., Perkin. Trans. I*, **1982**, 2735. (c) T. Shimazu and M. Yoshizawa, *J. Memb. Sci.*, 1983, **13**, 1. (d) M. Irie and M. Kato, *J. Am. Chem. Soc.*, 1985, **107**, 1024. (e) J. D. Winkler, K. Deshayes and B. Shao, *J. Am. Chem. Soc.*, 1989, **111**, 769.
- 4) M. Ino, J. Otsuki, K. Araki and M. Seno, *J. Membrane Sci.*, 1994, **89**, 101.
- 5) K. Araki, S.-K. Lee, J. Otsuki and M. Seno, *Chem. Lett.*, **1993**, 493.
- 6) K. Araki, S.-K. Lee and J. Otsuki, *J. Chem. Soc., Dalton Trans.*, in press.
- 7) S.-K. Lee, Y. Kumasaka, J. Otsuki and K. Araki, *Bull. Chem. Soc. Jpn.*, in press.
- 8) S.-K. Lee, H. Yamada, S. Mishina and K. Araki, *J. Chem. Soc., Chem. Commun.*, accepted.
- 9) M. Yamada, K. Araki and S. Shiraish, *Bull. Chem. Soc. Jpn.*, 1987, **60**, 3149; *ibid*, 1988, **61**, 2767.